Critical properties of a two-dimensional Ising magnet with quasiperiodic interactions

G. A. Alves,[1] M. S. Vasconcelos,[2] and T. F. A. Alves[3]
[1]*Departamento de Física, Universidade Estadual do Piauí, 59078-900, Teresina - PI, Brazil*
[2]*Escola de Ciências e Tecnologia, Universidade Federal do Rio Grande do Norte, 59078-900, Natal - RN, Brazil*
[3]*Departamento de Física, Universidade Federal do Piauí, 57072-970, Teresina - PI, Brazil*
(Received 19 October 2015; revised manuscript received 26 January 2016; published 12 April 2016)

We address the study of quasiperiodic interactions on a square lattice by using an Ising model with ferromagnetic and antiferromagnetic exchange interactions following a quasiperiodic Fibonacci sequence in both directions of a square lattice. We applied the Monte Carlo method, together with the Metropolis algorithm, to calculate the thermodynamic quantities of the system. We obtained the Edwards–Anderson order parameter q_{EA}, the magnetic susceptibility χ, and the specific heat c in order to characterize the universality class of the phase transition. We also use the finite size scaling method to obtain the critical temperature of the system and the critical exponents β, γ, and ν. In the low-temperature limit we obtained a spin-glass phase with critical temperature around $T_c \approx 2.274$, and the critical exponents β, γ, and ν, indicating that the quasiperiodic order induces a change in the universality class of the system. Also, we discovered a spin-glass ordering in a two-dimensional system which is rare and, as far as we know, the unique example is an under-frustrated Ising model.

DOI: 10.1103/PhysRevE.93.042111

I. INTRODUCTION

Since the discovery of quasicrystals by Shechtman *et al.* [1], awarded with the Nobel Prize, and the pioneering work of Merlin *et al.* [2] on the nonperiodic Fibonacci and Thue–Morse GaAs-AlAs superlattices, these quasiperiodic systems have attracted interest and hundreds of quasicrystals have been reported and confirmed. Quasicrystals are a particular type of solid that have a discrete point-group symmetry not present in Bravais lattices like a C_5 symmetry in two dimensions or icosahedral symmetry in three dimensions [3,4]. These systems can be viewed as intermediate between full translational symmetric systems and random amorphous solid systems [1] and possess a long-range structural order called quasiperiodicity. Some examples of such quasiperiodic systems are metallic alloys [5,6], soft-matter systems [7], supramolecular dendritic systems [8,9], and copolymers [10,11]. Quasiperiodic crystals have some unique properties, such as fractal spectra (in the case of exact solvable models) and localization of electronic [12,13] and photonic [14–16] states. Also, a model was proposed with localized spins [17] as an alternative way to simulate disorder.

In the last 30 years since their discovery, the study of quasicrystals significantly advanced our knowledge about the atomic scale structure [18,19], but many questions regarding the consequences of quasiperiodicity on physical properties, such as electronic and magnetic properties, remain open. One of the most interesting questions regarding magnetism in quasicrystals, yet unanswered, is whether long-range antiferromagnetic (AFM) order can be sustained in real quasicrystalline systems. A large number of theoretical studies have focused on the possibility of nontrivial ordering of localized magnetic moments on quasilattices [20–24] and have generally answered affirmatively. Nevertheless, to date, no quasi-antiferromagnets have been discovered. That is not to say that the low-temperature behavior of the known magnetic quasicrystals is uninteresting. Quite the contrary, they continue to offer new insights regarding the roles of topological order and frustration, as well as the microscopic nature of complex spin interactions in magnetic systems. This opens the opportunity to study new models to answer the open questions. For example, recently Tamura *et al.* [25] presented a theoretical model to explain the anomalous behavior in the susceptibility of Tb_6Cd, indicating that there is a possible antiferromagnetic phase transition. Therefore, the studies of the competing antiferromagnetic interactions in the two-dimensional (2D) Ising model with quasiperiodic interactions proposed here (in 2D) can give new insights in this field.

Indeed, by growth processes, one can control the amount of disorder and go from a long-range structural order situation to a quenched disorder [26,27] or, alternatively, to a quasiperiodic order by modifying the exchange strengths and signals. Quasiperiodic models, as far as we know, were not investigated in a systematic way. We are aware of a study of mean-field results of an Ising magnet with quasiperiodic interactions [28]. So, the main goal of this work is to obtain the thermodynamic properties of a Ising model in two dimensions with positive and negative exchange interactions with the same strength, ordered by a Fibonacci sequence in both directions of a square lattice.

This paper is organized as follows: In Sec. II we describe the model and the Hamiltonian, the results for the Edwards–Anderson order parameter q_{EA} [29], the magnetic susceptibility χ, the specific heat, and the critical behavior of the system are given in Sec. III, and, finally, we present some conclusions and general comments in Sec. IV.

II. MODEL AND SIMULATIONS

The most widely used model in the description of magnetic systems is the Ising model [30] which is given by the Hamiltonian

$$\mathcal{H} = -\sum_{\langle i,j \rangle} J_{ij} S_i S_j. \tag{1}$$

Here, S_i and S_j are the spin on sites i and j, respectively and their values can be ± 1. J_{ij} is the exchange interaction

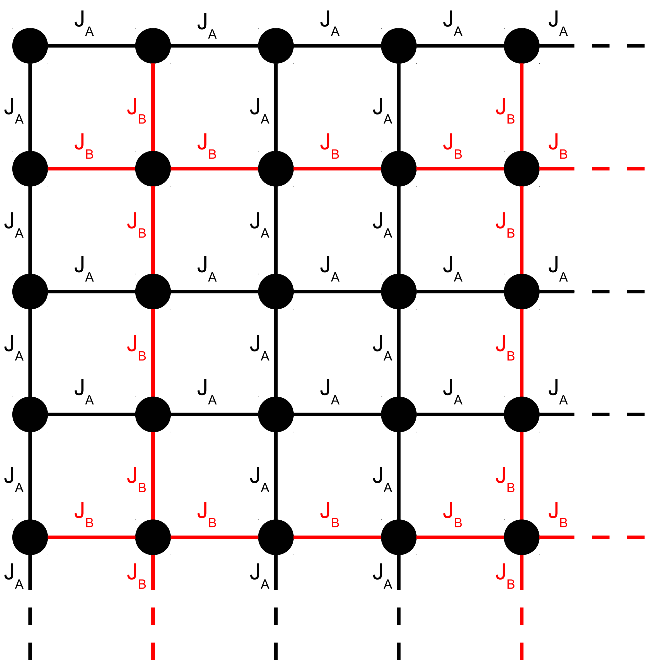

FIG. 1. Example of a lattice with quasiperiodic symmetry following the Fibonacci sequence. The red and blue lines stand for exchange interaction strengths $J_A = 1$ (ferromagnetic) and $J_B = -1$ (antiferromagnetic), respectively. We used the Fibonacci letter sequence, which is obtained from the substitution rules $A \to AB$ and $B \to A$ which means that, from one stage of the construction of the aperiodic sequence to the next, all letters A are replaced by AB and all letters B are replaced by A. Starting with the letter A, by repetitive applications of the substitution rule we can obtain the successive iterations of the Fibonacci sequence. The horizontal bonds follow a Fibonacci sequence in the vertical direction and similarly for the vertical bonds.

strength between first-neighbor spins S_i and S_j. The exchange constant can assume the values $J_A = 1$ and $J_B = -1$ in a particular spatial direction according to the respective letter in an aperiodic letter sequence. When J_{ij} is positive, we have a ferromagnetic interaction, conversely we have an antiferromagnetic interaction.

We used the Fibonacci letter sequence obtained from the substitution rules $A \to AB$ and $B \to A$, which means that from one stage of the construction of the aperiodic sequence to the next, all letters A are replaced by AB and all letters B are replaced by A. Starting with the letter A, by repetitive applications of the substitution rule we can obtain the successive iterations of the Fibonacci sequence. The exchange strengths follow the Fibonacci sequence at the two spatial directions of the square lattice. An example of such a lattice is shown in Fig. 1. To introduce competing interactions we considered the horizontal bonds following a Fibonacci sequence in the vertical direction and similarly for the vertical bonds.

These alternating ferromagnetic and antiferromagnetic interactions can generate competition between the spin interactions, and this has been studied both experimentally and theoretically. We can obtain spin-glass phases in these systems as shown by experimental evidence [10] for Mn and Fe impurities diluted in Cu and Au, inducing an effective coupling giving origin to the Ruderman–Kittel–Kasuya–Yosida interaction [9].

Theoretically, these systems with competitive interactions were investigated by using the Edwards–Anderson (EA) model [29]. It is worth mentioning that the EA model originally considered a Gaussian distribution of strengths J_{ij} in a d-dimensional lattice with nearest-neighbor interactions similar to the Ising model. The most important result of this model is the presence of a spontaneous symmetry breaking leading to an ordered phase in the low-temperature limit, called the spin-glass phase. In a spin-glass phase the spin at a particular site has a nonzero mean value $m_i = \langle S_i \rangle$; however, the total magnetization is zero.

We generated an initial random spin configuration $S_i = \pm 1$ in a square lattice and used the Metropolis algorithm for the Monte Carlo method (MCM) [31] to generate the steady-state configurations. In this way, we determined the EA order parameter $\langle q_{\text{EA}} \rangle$ [29], the susceptibility χ, the specific heat c, and Binder cumulant g_L [32], defined by the following relations:

$$q_{\text{EA}} = \frac{1}{N} \sum_{i,j} S_{i,j}^2, \tag{2}$$

$$\chi = N\left(\left\langle q_{\text{EA}}^2 \right\rangle - \langle q_{\text{EA}} \rangle^2\right)/T, \tag{3}$$

$$c = N(\langle H^2 \rangle - \langle H \rangle^2)/T^2, \tag{4}$$

$$g_L = \frac{1}{2}\left(3 - \frac{\left\langle q_{\text{EA}}^4 \right\rangle}{\left\langle q_{\text{EA}}^2 \right\rangle^2}\right), \tag{5}$$

respectively. Here $\langle \cdots \rangle$ stands for a thermal average over sufficiently many independent steady-state-system configurations and L and T are the lattice size and the absolute temperature, respectively. We used the following values of the lattice size L: 5, 8, 13, 21, 34, 55, 89, 144, 233, 377, and 610, which are the first Fibonacci numbers. The total number of spins for each lattice size is L^2.

The thermodynamic properties are functions of the temperature T and they obey the following finite size scaling (FSS) relations [33]:

$$q_{\text{EA}} = L^{-\beta/\nu} f_q(\vartheta), \tag{6}$$

$$\chi = L^{\gamma/\nu} f_\chi(\vartheta), \tag{7}$$

$$c = L^{\alpha/\nu} f_c(\vartheta), \tag{8}$$

where β, γ, α, and ν are the usual critical exponents and $f_i(\vartheta)$ are the FSS functions with

$$\vartheta = L^{1/\nu}|T - T_c| \tag{9}$$

being the scaling variable. Therefore, from the lattice-size dependence of the EA parameter q_{EA} and the susceptibility χ we obtained the critical-exponent ratios β/ν and γ/ν, respectively. Following the scaling-variable dependence, we expect that the susceptibility maxima T_χ scales with the system size L as

$$T_\chi = T_c + bL^{-1/\nu}, \tag{10}$$

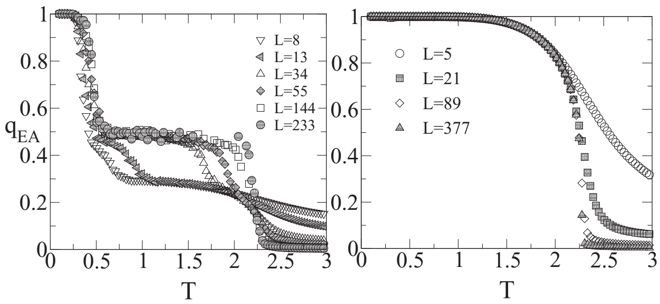

FIG. 2. Edwards–Anderson order parameter q_{EA} versus temperature T for different lattice sizes L and periodic boundary conditions. The values of L obey the Fibonacci sequence. For some lattice sizes we observe the presence of *plateaus* on q_{EA} which are a finite-size effect. These *plateaus* are absent for open boundary conditions or higher lattice sizes. Therefore, in all other results presented in this work we use only open boundary conditions.

where $b \approx 1$. Therefore, the susceptibility maxima T_χ as a function of system size L can be used to evaluate the exponent $-1/\nu$.

We used 1×10^6 MCM steps to make the system reach the steady state and the independent steady-state system configurations are estimated in the next 1×10^5 MCM steps. One MCM step is accomplished when all N spins are investigated if they flip or not. We carried out 10^3 independent steady-state configurations to calculate the needed thermodynamic averages.

III. RESULTS AND DISCUSSION

We investigated first the influence of lattice boundary conditions on thermodynamic properties. We show the EA order parameter q_{EA} given by Eq. (2) as a function of temperature T in Fig. 2 for periodic boundary conditions. We observe the presence of *plateaus* on q_{EA} which are a finite-system-size effect. These *plateaus* are absent in open boundary conditions in all lattice sizes and in the high-lattice-size limit we do not observe these *plateaus* for either boundary conditions. Therefore, in all other results presented in this work we use only open boundary conditions.

To study the critical behavior of the system we evaluated the Binder cumulant g_L given by Eq. (5) in order to obtain the critical temperature. We show the Binder cumulant in Fig. 3. The critical temperature T_c is estimated as the point where the curves for different size lattices intercept each other. We obtained $T_c \approx 2.274$.

The correspondent behavior of the EA parameter q_{EA} versus temperature T is presented in Fig. 4. The q_{EA} dependence suggests the presence of a second-order phase transition in the system. The phase transition occurs at the critical temperature $T_c \approx 2.274$. The critical behavior given by Eq. (6) of the EA order parameter is shown in Fig. 5. The slope of the curve corresponds to the exponent ratio $\beta/\nu = 0.40\,(2)$. The exponent ratio differs from the pure model and this change of the universality class is induced by the quasiperiodic order.

It is well known that, if the model has a continuous transition in its full translational symmetric version, the influence of random interactions on their critical behavior is summarized by

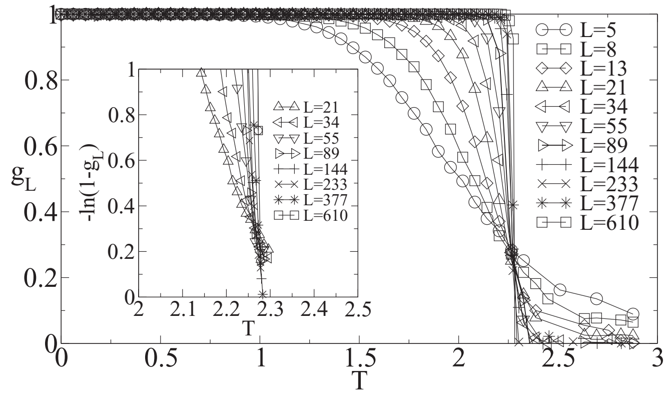

FIG. 3. Binder cumulant g_L versus temperature T for different lattice sizes L. The values of L obey the Fibonacci sequence. We estimated the critical temperature $T_c \approx 2.274$ by averaging the numerical values of the temperatures where the curves intersect each other. We have, for this model, a phase transition from a paramagnetic phase to a spin-glass phase by decreasing the temperature.

the Harris criterion [34], which establishes that, if $2 - d\nu < 0$ where d is the spatial dimensionality, the quenched disorder will not change the critical behavior of the system and it is said to be irrelevant. However, the Harris criterion is not valid at the random system criticality [35] where $\phi < \alpha$ for the random model, as known from perturbative expansions where $\phi = 2 - d\nu$ is the crossover exponent. For the pure model, the equality $\phi = \alpha$ is restored.

By the inequality involving α and ϕ, it is possible, at least in theory, to have a model with α positive and ϕ negative, in a way the random system will have the same critical behavior as the pure model. However, there are no systems reported with such behavior as far as we know. In our case, we have $\phi = 0$, as we show later. In this way, we can expect a different critical behavior and different exponents from the Ising 2D exponents.

The Luck criterion for the quasiperiodic ordered model, analogous to the Harris criterion for the random disordered model, establishes that, if the ϕ exponent is positive, the critical behavior of the quasiperiodic model differs from the fully translational symmetric model and the disorder is called relevant. Conversely, if ϕ is negative, the critical behavior is the

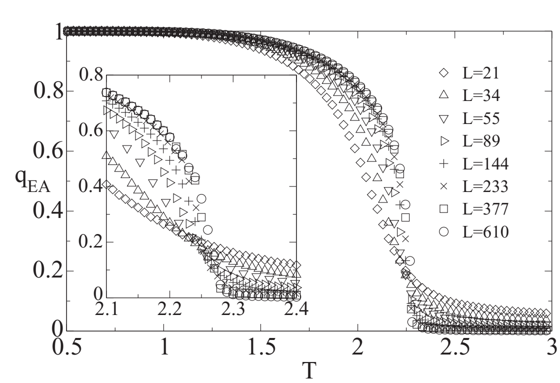

FIG. 4. The EA order parameter q_{EA} as a function of temperature T for different lattice sizes L. The values of L obey the Fibonacci sequence. The curves suggest a second-order phase transition.

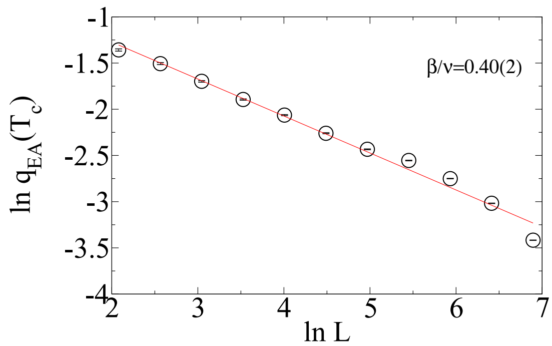

FIG. 5. Critical behavior of q_{EA} at $T = T_c$ as a function of lattice size L obtained from Eq. (6). Alongside the q_{EA} points we show the error bars on the same scale. The curve slope gives the exponent ratio $\beta/\nu = 0.40\,(2)$. This exponent ratio differs from that of the pure model and this change in universality class is induced by the quasiperiodic order.

same of the pure model and the disorder is called irrelevant. On the marginal case $\phi = 0$ we obtained a change of the universality class of the model as observed, for example, in mean-field results for an Ising model in a hypercubic lattice [28].

To obtain an explicit expression for the crossover exponent, we can follow Refs. [36–38] to express the total number of exchange interactions and the fluctuations between the frequencies of the ferromagnetic and antiferromagnetic interactions between the n-esimal generation of the lattice and the semi-infinite lattice scales with the total length of the system L as

$$J \propto N \propto L, \tag{11}$$

$$\Delta J \propto \Delta N \propto L^{\omega}, \tag{12}$$

where ω and J are, respectively, the geometrical wandering exponent of the lattice and the total exchange strength. The critical temperature T_c is proportional to J, so we can write

$$\delta t = \frac{\Delta J}{J} \sim L^{\omega-1}, \tag{13}$$

where $t = (T - T_c)/T_c$ is the reduced temperature and δt stands for the fluctuations on the reduced temperature when we introduce the aperiodicity. Combining Eq. (13) with the scaling form $L \sim \varepsilon \sim t^{-\nu}$ for the pure model (ε is the correlation length), we have

$$\frac{\delta t}{t} = t^{-1-\nu(\omega-1)}, \tag{14}$$

and by using the expression $\frac{\delta t}{t} \sim t^{-\phi}$, we obtain the crossover exponent

$$\phi = 1 + \nu(\omega - 1), \tag{15}$$

which is the same expression obtained in Ref. [36]. In our case, $\nu = 1$ for the uniform model.

To evaluate the crossover exponent, we need the wandering exponent for our lattice. To accomplish this task we note that the 2D lattice showed in Fig. 1 can be generated by the geometric recursive substitutions of the lattice monomers shown

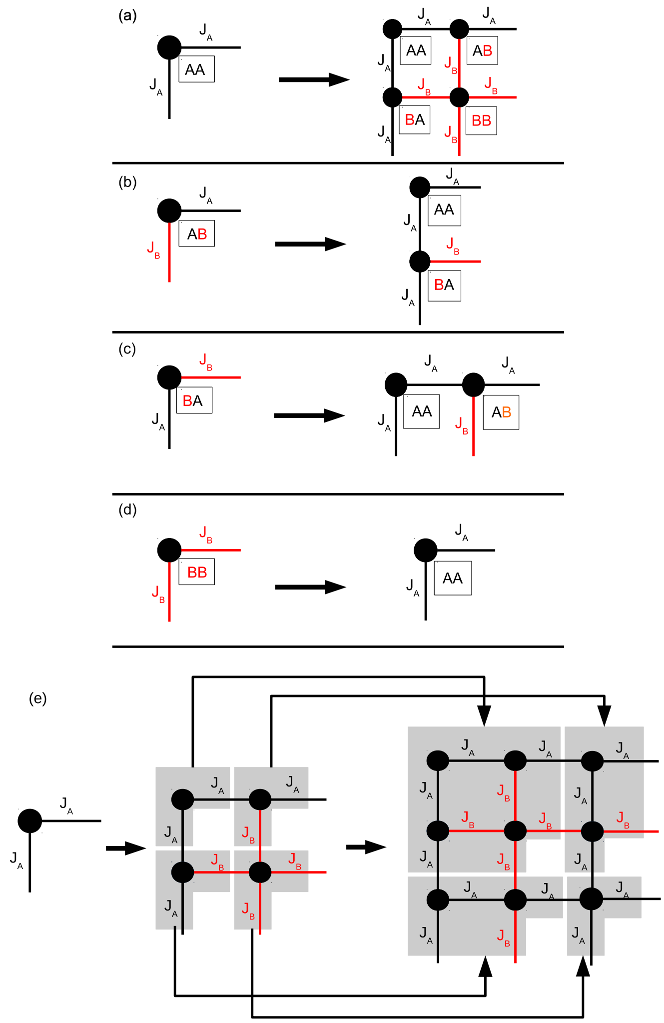

FIG. 6. Starting from the lattice monomer in panel (a), we can obtain the successive generations of the lattice in Fig. 1 by applying the recursive geometrical substitutions presented in panels (a)–(d) which are formally equivalent to the respective substitution rules $(AA) \to (AA)(AB)(BA)(BB)$, $(AB) \to (AA)(BA)$, $(BA) \to (AA)(AB)$, and $(BB) \to (AA)$. In panel (e) we show the first three generations of our lattice by applying the geometrical substitution rules presented in panels (a)–(d).

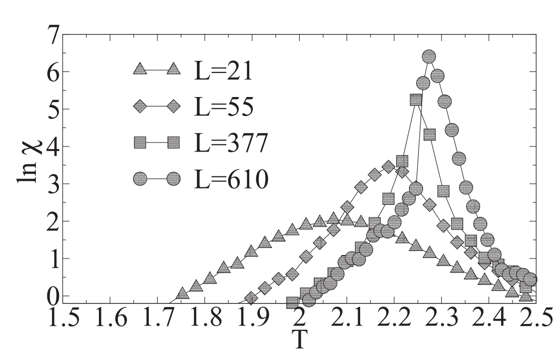

FIG. 7. The susceptibility χ as function of temperature T for different lattice sizes L. The values of L obey the Fibonacci sequence. The susceptibility diverges at T_c in the large-lattice-size limit, suggesting a second-order phase transition.

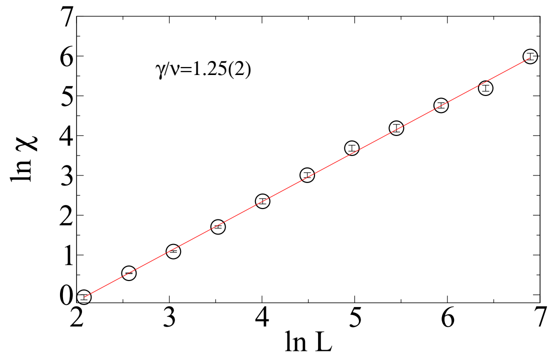

FIG. 8. Critical behavior of χ at $T = T_c$ as a function of lattice size L obtained from Eq. (7). Alongside the χ points we show the error bars on the same scale. The curve slope gives the exponent ratio $\gamma/\nu = 1.25\,(2)$, differing from the pure Ising 2D case.

in Fig. 6, starting with the monomer shown in Fig. 6(a). The recursive geometrical substitutions are formally equivalent to the substitution rules $(AA) \to (AA)(AB)(BA)(BB)$, $(AB) \to (AA)(BA)$, $(BA) \to (AA)(AB)$, and $(BB) \to (AA)$. Therefore, we can write the following substitution matrix for the substitution rules:

$$\mathcal{M} = \begin{pmatrix} 1 & 1 & 1 & 1 \\ 1 & 0 & 1 & 0 \\ 1 & 1 & 0 & 0 \\ 1 & 0 & 0 & 0 \end{pmatrix}. \tag{16}$$

The substitution matrix connects the number of the four possible letter pairs between the $n+1$ and n-esimal generations of the lattice. The above substitution rules are analogous to four-letter inflation rules. The $\mathcal{M}$ eigenvalues are given by $\lambda_1 = \varphi^2$, $\lambda_2 = \lambda_3 = -1$, and $\lambda_4 = 1/\varphi^2$, where $\varphi = \frac{1+\sqrt{5}}{2}$ is the golden ratio. The wandering exponent is given by the following expression [37]:

$$\omega = \frac{\ln|\lambda_2|}{\ln(\lambda_1)}, \tag{17}$$

where λ_1 and λ_2 are the leading and the next-to-leading eigenvalues (in moduli) of the substitution matrix $\mathcal{M}$. By using the eigenvalues of $\mathcal{M}$ we evaluated $\omega = 0$ and from Eq. (15) we obtained $\phi = 0$. Therefore, our lattice has marginal fluctuations according to the Harris–Luck criterion [37] and we can expect a change in the universality class.

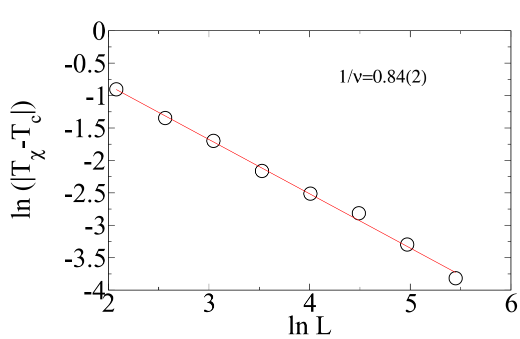

FIG. 9. Critical behavior of susceptibility maxima temperatures T_χ as function of lattice size L obtained from Eq. (10). The curve slope gives the exponent $1/\nu = 0.84\,(2)$, differing from the pure Ising 2D case.

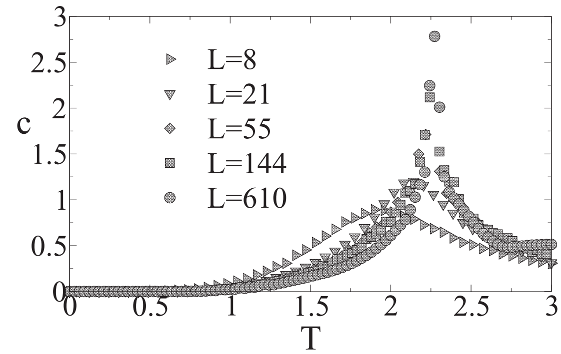

FIG. 10. Specific heat c as function of temperature T for different lattice sizes L. The values of L obey the Fibonacci sequence. When increasing the lattice size we observe a crescent maxima, suggesting a logarithmic divergence or a negative-exponent divergence at the critical temperature $T_c \approx 2.274$.

We present the susceptibility χ as a function of temperature T in Fig. 7. In the large-lattice-size limit, the susceptibility diverges at $T_c \approx 2.274$. The FSS critical behavior of χ, given by Eq. (7), is presented in Fig. 8. The slope of the curve gives the critical-exponent ratio $\gamma/\nu = 1.25\,(2)$. The exponent ratio differs from the pure model and this change in the universality class is induced by the quasiperiodic order.

To obtain the critical exponent $1/\nu$, we investigated the critical behavior of the temperatures T_χ for which the susceptibility is maximal. We show the critical behavior of T_χ in Fig. 9. The critical behavior obeys Eq. (10) and from the slope of the curve we obtain the value of the exponent $1/\nu = 0.84\,(2)$, which differs from the pure Ising 2D case. The quasiperiodic order induces a change in the universality class of the system.

We show the specific heat c, given by Eq. (4), in Fig. 10. The curves suggest a critical behavior as a function of T. When increasing the lattice size we observe a crescent maxima, suggesting a logarithm divergence or a negative exponent divergence at the critical temperature. We estimate the α exponent by collapsing the specific heat c for different lattice sizes following the scaling relation presented in Eq. (8). Our best data collapsing, presented in Fig. 11, was obtained for $\alpha/\nu \approx -0.40$.

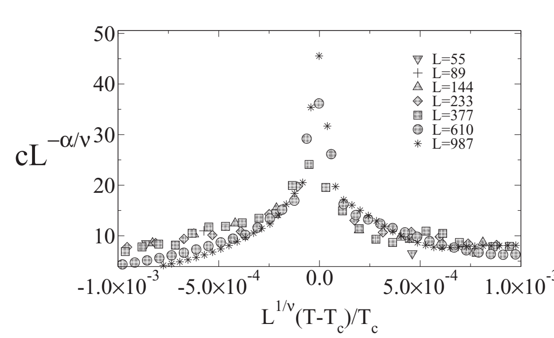

FIG. 11. Data collapse of specific heat c for different lattice sizes L. The best data collapsing gives us the estimate $\alpha/\nu \approx -0.40$.

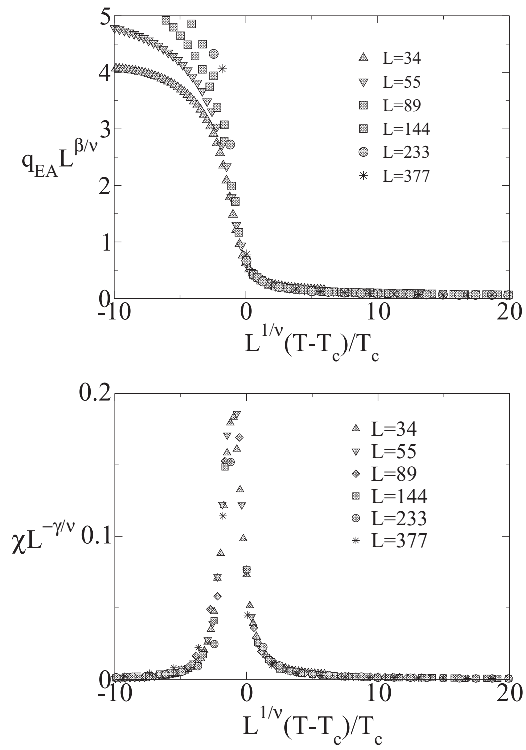

FIG. 12. Data collapse of EA order parameter q_{EA} and susceptibility χ. The thermodynamic parameters as functions of lattice size collapse for $\beta/\nu = 0.40\,(2)$, $\gamma/\nu = 1.25\,(2)$, and $1/\nu = 0.84\,(2)$ next to the critical temperature according to the scale forms given in Eq. (6) differing from the pure Ising 2D case.

Finally, we show our data collapsed to confirm the obtained exponents β, γ, and ν. We see, from Fig. 12, that all the data for the EA order parameter q_{EA} and the susceptibility χ as a function of lattice sizes collapse for $\beta/\nu = 0.40\,(2)$ and $1/\nu = 0.84\,(2)$, next to the critical temperature according to the correspondent scale forms given in Eq. (6) for a second-order phase transition. We have for this system a second-order phase transition from a paramagnetic phase to a spin-glass phase by decreasing the temperature. We would like to emphasize that the exponent ratios obtained differ from the Ising 2D ones, changing the universality class of the system.

IV. CONCLUSIONS

We presented a simple model with quasiperiodic long-range order with competing interactions and obtained the critical behavior of a second-order transition in the Edwards–Anderson parameter driven by temperature. In the low-temperature limit we obtained a spin-glass phase with critical temperature $T_c \approx 2.274$. The spin-glass ordering in a two-dimensional system is rare and, as far as we know, the only other example is an under-frustrated Ising model [39].

We obtained the critical exponents β, γ, and ν in the case of equal antiferromagnetic and ferromagnetic strengths. The values of the exponents β/ν, γ/ν, and $1/\nu$ are 0.40 (2), 1.25 (2), and 0.84 (2) respectively. Our result for $\beta = 0.48\,(2)$ is interesting because it is the same for the Landau classic theory of second-order phase transitions. The exponents obtained differ from Ising 2D exponents so the quasiperiodic order can change the universality class of the model. Therefore, the quasiperiodic ordering changes the critical behavior in the 2D case.

ACKNOWLEDGMENTS

We would like to thank CNPq (Conselho Nacional de Desenvolvimento Científico e tecnológico) and FAPEPI (Fundação de Amparo a Pesquisa do Estado do Piauí) for the financial support. We acknowledge the use of the High-Performance Computer System of the International Institute of Physics - UFRN, Natal, Brazil, and Dietrich Stauffer Computational Physics Lab - UFPI, Teresina, Brazil where the numerical simulations were performed.

[1] D. Shechtman, I. Blech, D. Gratias, and J. W. Cahn, Phys. Rev. Lett. **53**, 1951 (1984).
[2] R. Merlin, K. Bajema, R. Clarke, F. Y. Juang, and P. K. Bhattacharya, Phys. Rev. Lett. **55**, 1768 (1985).
[3] H. C. Jeong and P. J. Steinhardt, Phys. Rev. B **48**, 9394 (1993).
[4] D. Levine and P. J. Steinhardt, Phys. Rev. Lett. **53**, 2477 (1984).
[5] W. Steurer, Chem. Soc. Rev. **41**, 6719 (2012).
[6] E. Maciá, Rep. Prog. Phys. **69**, 397 (2006).
[7] S. Fischer, A. Exner, K. Zielske, J. Perlich, S. Deloudi, W. Steurer, P. Lindner, and S. Förster, Proc. Natl. Acad. Sci. USA **108**, 1810 (2011).
[8] X. Zeng, G. Ungar, Y. Liu, V. Percec, A. E. Dulcey, and J. K. Hobbs, Nature (London) **428**, 157 (2004).
[9] X. Zeng, Curr. Opin. Colloid Interface Sci. **9**, 384 (2005).
[10] A. Takano, W. Kawashima, A. Noro, Y. Isono, N. Tanaka, T. Dotera, and Y. Matsushita, J. Polym. Sci., Part B: Polym. Phys. **43**, 2427 (2005).
[11] K. Hayashida, T. Dotera, A. Takano, and Y. Matsushita, Phys. Rev. Lett. **98**, 195502 (2007).
[12] M. Vasconcelos, P. Mauriz, U. Fulco, and E. Albuquerque, Phys. Lett. A **363**, 322 (2007).
[13] M. S. Vasconcelos, D. L. Azevedo, A. Hadad, and D. S. Galvo, J. Phys.: Condens. Matter **23**, 405501 (2011).
[14] M. S. Vasconcelos and E. L. Albuquerque, Phys. Rev. B **57**, 2826 (1998).
[15] M. S. Vasconcelos and E. L. Albuquerque, Phys. Rev. B **59**, 11128 (1999).
[16] M. S. Vasconcelos, P. W. Mauriz, F. F. de Medeiros, and E. L. Albuquerque, Phys. Rev. B **76**, 165117 (2007).
[17] R. F. S. Andrade and S. T. R. Pinho, Eur. Phys. J. B **34**, 343 (2003).
[18] W. Steurer and S. Deloudi, Acta Crystallogr., Sect. A: Found. Crystallogr. **64**, 1 (2008).
[19] A.-P. Tsai, Chem. Soc. Rev. **42**, 5352 (2013).
[20] A. Jagannathan, Phys. Rev. Lett. **92**, 047202 (2004).

[21] E. Y. Vedmedenko, U. Grimm, and R. Wiesendanger, Phys. Rev. Lett. **93**, 076407 (2004).
[22] S. Matsuo, S. Fujiwara, H. Nakano, and T. Ishimasa, J. Non-Cryst. Solids **334-335**, 421 (2004).
[23] A. Jagannathan, Phys. Rev. B **71**, 115101 (2005).
[24] E. Y. Vedmedenko, U. Grimm, and R. Wiesendanger, Philos. Mag. **86**, 733 (2006).
[25] R. Tamura, Y. Muro, T. Hiroto, K. Nishimoto, and T. Takabatake, Phys. Rev. B **82**, 220201 (2010).
[26] Z.-Y. Li, X. Zhang, and Z.-Q. Zhang, Phys. Rev. B **61**, 15738 (2000).
[27] V. A. Shchukin and D. Bimberg, Rev. Mod. Phys. **71**, 1125 (1999).
[28] T. P. Oliveira and N. S. Branco, Phys. Rev. E **85**, 011113 (2012).
[29] S. F. Edwards and P. W. Anderson, J. Phys. F: Met. Phys. **5**, 965 (1975).
[30] E. Ising, Z. Phys. **31**, 253 (1925).
[31] N. Metropolis, A. Rosenbluth, M. Rosenbluth, A. Teller, and E. Teller, J. Chem. Phys. **21**, 1087 (1953).
[32] K. Binder, Phys. Rev. Lett. **47**, 693 (1981).
[33] F. W. S. Lima, Physica A (Amsterdam, Neth.) **391**, 1753 (2012).
[34] M. S. Faria, N. S. Branco, and M. H. R. Tragtenberg, Phys. Rev. E **77**, 041113 (2008).
[35] D. Andelman and A. N. Berker, Phys. Rev. B **29**, 2630 (1984).
[36] F. Iglói and L. Turban, Europhys. Lett. **27**, 91 (1994).
[37] J. M. Luck, Europhys. Lett. **24**, 359 (1993).
[38] S. T. R. Pinho, T. A. S. Haddad, and S. R. Salinas, Braz. J. Phys. **27**, 567 (1997).
[39] E. Ilker and A. N. Berker, Phys. Rev. E **89**, 042139 (2014).